AGU PUBLICATIONS

JGR

Journal of Geophysical Research: Oceans

RESEARCH ARTICLE

10.1002/2015JC010781

Key Points:
- CFC and SF6 constrained transit time distributions (TTDs)
- TTDs and AOU indicate steady ventilation of subtropics 1994–2007/2008
- Depth-integrated O_2 demand indicates C-export of 2–3.5 moles C m^{-2} yr^{-1}

Correspondence to:
R. E. Sonnerup,
rolf@u.washington.edu

Citation:
Sonnerup, R. E., S. Mecking, J. L. Bullister, and M. J. Warner (2015), Transit time distributions and oxygen utilization rates from chlorofluorocarbons and sulfur hexafluoride in the Southeast Pacific Ocean, *J. Geophys. Res. Oceans*, *120*, 3761–3776, doi:10.1002/2015JC010781.

Received 24 FEB 2015
Accepted 24 APR 2015
Accepted article online 29 APR 2015
Published online 27 MAY 2015

Transit time distributions and oxygen utilization rates from chlorofluorocarbons and sulfur hexafluoride in the Southeast Pacific Ocean

Rolf E. Sonnerup[1,2], Sabine Mecking[3], John L. Bullister[2], and Mark J. Warner[4]

[1]Joint Institute for Study of the Atmosphere and Ocean, University of Washington, Seattle, Washington, USA, [2]Pacific Marine Environmental Laboratory, National Oceanic and Atmospheric Administration, Seattle, Washington, USA, [3]Applied Physics Laboratory, University of Washington, Seattle, Washington, USA, [4]School of Oceanography, University of Washington, Seattle, Washington, USA

Abstract Chlorofluorocarbons-11 (CFC-11), CFC-12, and sulfur hexafluoride (SF_6) were measured during the December 2007 to February 2008 CLIVAR/Repeat Hydrography (RH) P18 section along ~103°W in the Southeast Pacific Ocean. Transit-time distributions (TTDs) of 1-D transport that matched all three tracers were consistent with high Peclet number flow ventilating the subtropical mode water and the main subtropical thermocline (30°S–42°S, 200–800 m). In the subtropics, TTDs with predominantly advective transport predicted decadal increases in CFC-12 and CFC-11 consistent with those observed comparing 1994 WOCE with 2007/2008 CLIVAR/RH data, indicating steady ventilation in this region, and consistent with the near-zero changes observed in dissolved oxygen. The mean transport timescales from the tracer-tuned TTDs were used to estimate apparent oxygen utilization rates (OURs) on the order of 8–20 μmol kg^{-1} yr^{-1} at ~200 m depth, attenuating to ~2 μmol kg^{-1} yr^{-1} typically by 500 m depth in this region. Depth-integrated over the thermocline, these OURs implied carbon export rates from the overlying sea surface on the order of ~1.8 moles C m^{-2} yr^{-1} from 30°S to 45°S, 2–2.5 moles C m^{-2} yr^{-1} from 45°S to 52°S, and 2.5–3.5 moles C m^{-2} yr^{-1} from 52°S to 60°S.

1. Introduction

Since the mid-1990s, the atmospheric growth rates of the chlorofluorocarbons (CFCs) CFC-11 and CFC-12 have slowed and, recently, reversed (Figure 1). This means that shallow (usually < 350 m) waters can no longer be confidently dated simply using CFC concentrations. Sulfur hexafluoride (SF_6) is another anthropogenic trace gas whose atmospheric concentration has been increasing rapidly over the past four decades (Figure 1), providing a useful water mass dating tool in upper ocean waters [*Bullister et al.*, 2006; *Tanhua et al.*, 2008]. All of the U.S. and many international CFC measurement groups have modified their analytical equipment to also include dissolved SF_6 on CLIVAR/Repeat Hydrography (RH) program sections. SF_6 provides a useful replacement for the CFCs near the sea surface and, because its atmospheric history is independent from those of the CFCs, SF_6 can provide additional information useful for estimating the impacts that mixing in the ocean interior has on the tracer ages [*Waugh et al.*, 2002, 2003]. In this way, the complementary temporal information available from SF_6 improves our confidence in the use of CFCs to estimate anthropogenic CO_2 accumulation [*Hall et al.*, 2002; *Bullister et al.*, 2006] and oxygen utilization [*Sonnerup et al.*, 2013] rates in the thermocline and to diagnose changes in oceanic ventilation [*Waugh et al.*, 2003, 2013; *Sonnerup et al.*, 2008].

In this effort, we use the CFCs/SF_6 tracer combination to estimate transit time distributions (TTDs) in the ocean interior on a meridional section occupied along 103°W in the SE Pacific Ocean during 2007/2008, the CLIVAR/RH P18 line. These data were reported to precision not previously attained for the CFCs and SF_6, with implications for the TTDs implied. Because this section was a repeat of the 1994 WOCE line, we use temporal changes in CFCs as an additional constraint on the TTDs [*Waugh et al.*, 2003]. We then use the tracer-derived transport timescales from the sea surface to estimate thermocline oxygen utilization rates, and implied organic carbon remineralization rates, along the P18 line in the subtropical and subantarctic Southeast Pacific Ocean.

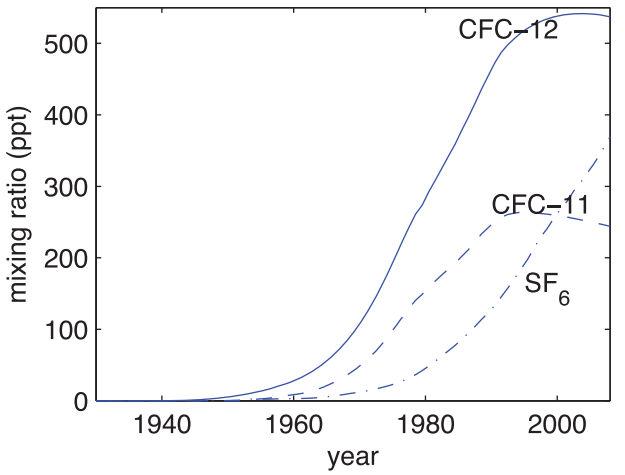

Figure 1. Concentrations of CFC-12, CFC-11, and SF_6 (*60) in the Southern Hemisphere troposphere during 1930–2009, reconstructed as outlined in *Bullister* [2015].

2. Tracer Measurements Along ~103°W

Dissolved CFC-11, CFC-12, and SF_6 were measured using analytical techniques outlined in *Bullister and Wisegarver* [2008] during the December 2007 to February 2008 (2007/2008) CLIVAR/RH reoccupation of the WOCE P18 line along 110°W in the North and Equatorial Pacific to 5°S, and along 103–105°W between 10°S and 70°S (Figure 2). Detection limits for the CFCs and for SF_6 were approximately 0.001 pmol kg^{-1} and 0.01 fmol kg^{-1}, respectively. Based on replicate samples, we estimated the measurement precision as the larger of $\pm$ 0.015 fmol kg^{-1} or 2.2% for SF_6, $\pm$ 0.0045 pmol kg^{-1} or 0.5% for CFC-11, and $\pm$ 0.0025 pmol kg^{-1} or 0.4% for CFC-12. We also made use of the WOCE P18 line occupied along approximately the same cruise track during January–April 1994. These earlier data included only the CFCs, to somewhat lower precision, 1% or 0.005 pmol kg^{-1}, whichever is larger, and with higher detection limit, ~0.004 pmol kg^{-1}. The differences in detection limit and precision result primarily from an increase in the volume of the sample analyzed. In order to also measure SF_6, approximately 200 cm^3 water samples were analyzed in 2007/2008, as compared to the 35 cm^3 sample size used for CFC-only analyses in 1994.

At the northern end of the 2007/2008 P18 section, CFC-12 (CFC-11 as well, but not shown) and SF_6 were detectable throughout much of the water column (Figure 3). These samples were collected at the beginning of the cruise section, so we cannot rule out the possibility of bottle contamination. However, previous measurements of the CFCs in this region of the eastern North Pacific over the past three decades have detected a relatively constant near-bottom feature. *Min et al*. [2002] hypothesize that these elevated concentrations derive not from ventilation, but from some process involving scavenging onto particles and subsequent release from the sediments. Dumping of CFC or SF_6 containing materials from ships in this heavily trafficked region, followed by release of these compounds, is another possible source for the anomalous CFC and SF_6 signals observed at depth.

At the sea surface, saturation levels of both CFC-11 and CFC-12 with respect to the atmospheric CFC concentrations [*Bullister*, 2015] were on the order of 5–10% supersaturated from 40°S to 10°S (Figure 4). Supersaturation of these compounds with slightly higher CFC-11 than CFC-12 saturations during the summer are consistent with the rate of decrease in equilibrium concentrations resulting from seasonal warming exceeding the rate at which air-sea exchange can reequilibrate the sea surface [*Warner and Weiss*, 1992; *Warner et al*., 1996]. SF_6 exhibited the same degree of saturation with respect to atmospheric equilibrium. The larger scatter for SF_6 reflects the lower precision of the measurement relative to its equilibrium concentration, a result of very low SF_6 levels in the atmosphere and its relatively low solubility in seawater [*Bullister et al*., 2002].

The reported sea surface saturation levels (Figure 4) were measured during summer 2007/2008, while subsurface water parcels were likely subducted into the ocean interior during wintertime [*Stommel*, 1979]. An estimate of the wintertime sea surface saturation levels is required for interpreting the distributions of these compounds in the ocean interior. Wintertime saturation can be significantly different from 100% in the Southeast Pacific due to the very deep mixed layers that form there [*Hartin et al*., 2011]. We estimated "outcropping" saturation levels for individual density classes from the CLIVAR/RH P18 section's CFC and SF_6 saturation state in remnant winter mixed layers as a function of latitude (Table 1). Outcropping locations and wintertime mixed layer depths were estimated from World Ocean Atlas climatology [*Conkright et al*., 2002]. On shallower isopyncals (σ_θ <27.0), saturation levels for CFC-11 were ~ 2% higher than for CFC-12 and SF_6, possibly due in part to the recent decreases in atmospheric CFC-11 levels. On the deepest isopycnals, SF_6

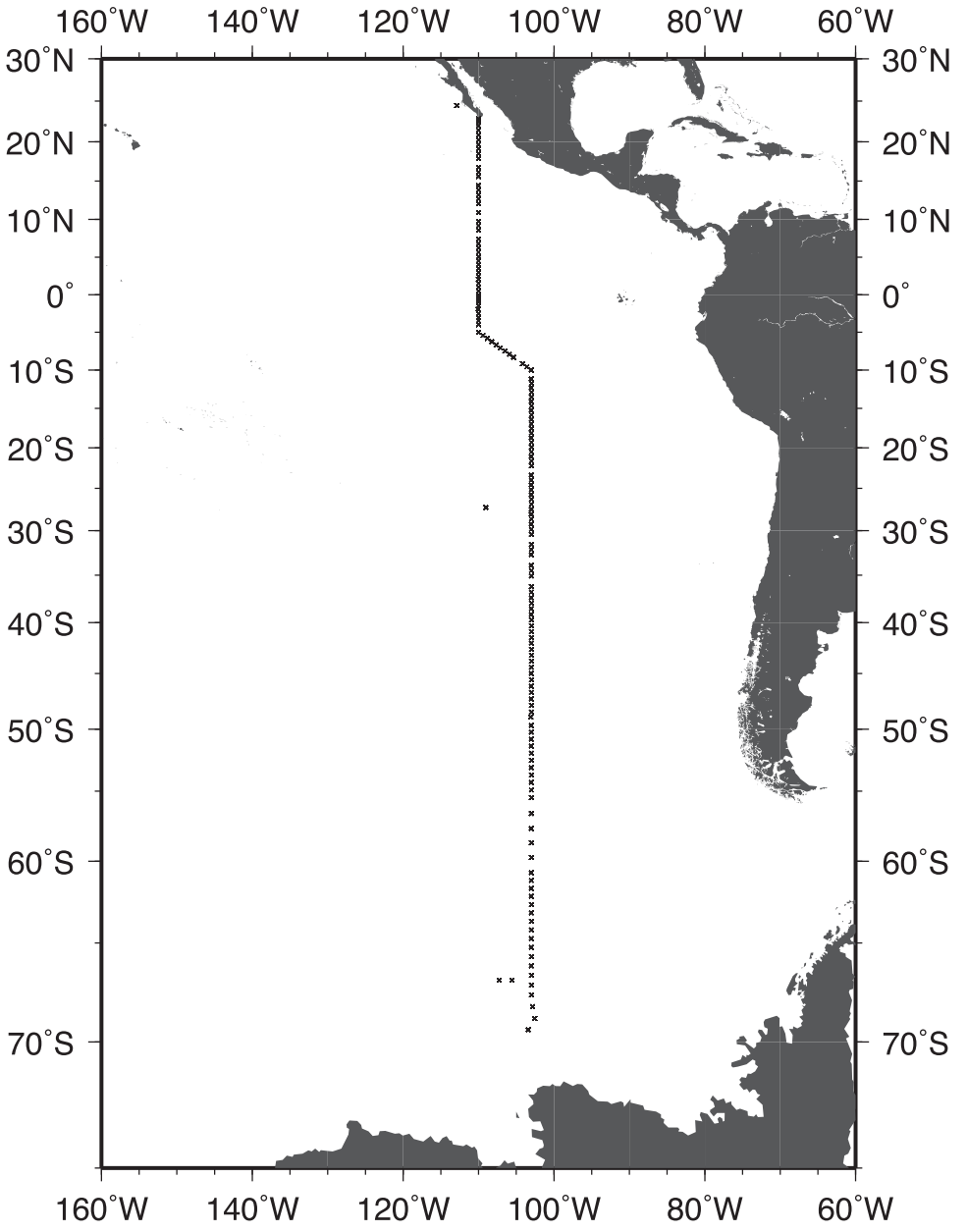

Figure 2. Locations where depth profiles of CFCs and SF_6 were collected during the 2007/2008 CLIVAR/RH reoccupation of the P18 line.

saturation was a bit lower than both CFCs, consistent with the recent rapid growth of SF_6 in the atmosphere [*Shao et al*., 2013].

Partial pressure ages for the CFCs (*p*CFC ages) and SF_6 (pSF_6 ages) were determined by (1) calculating the partial pressure of each subsurface sample by dividing its dissolved tracer concentration by the tracer solubility function [*Warner and Weiss*, 1985; *Bullister et al*., 2002] at the measured temperature and salinity, (2) comparing the partial pressure with the atmospheric histories (Figure 1) and (3) assigning a date that the sample was last at the surface by assuming the saturations determined above (Table 1) with respect to the atmosphere at that time [*Bullister*, 1989]. For waters younger than 14 years in 2007/2008, the concurrent pSF_6 measurement was used to distinguish pre and post-1994 vintages in determining the pCFC-11 ages [*Sonnerup et al*., 2008]. However, since the decrease in atmospheric CFC-11 levels after 1994 (Figure 1) has been slow relative to measurement and saturation level uncertainties, pCFC-11 ages $<$ 18 years could not be determined to better than $\pm$ 25%.

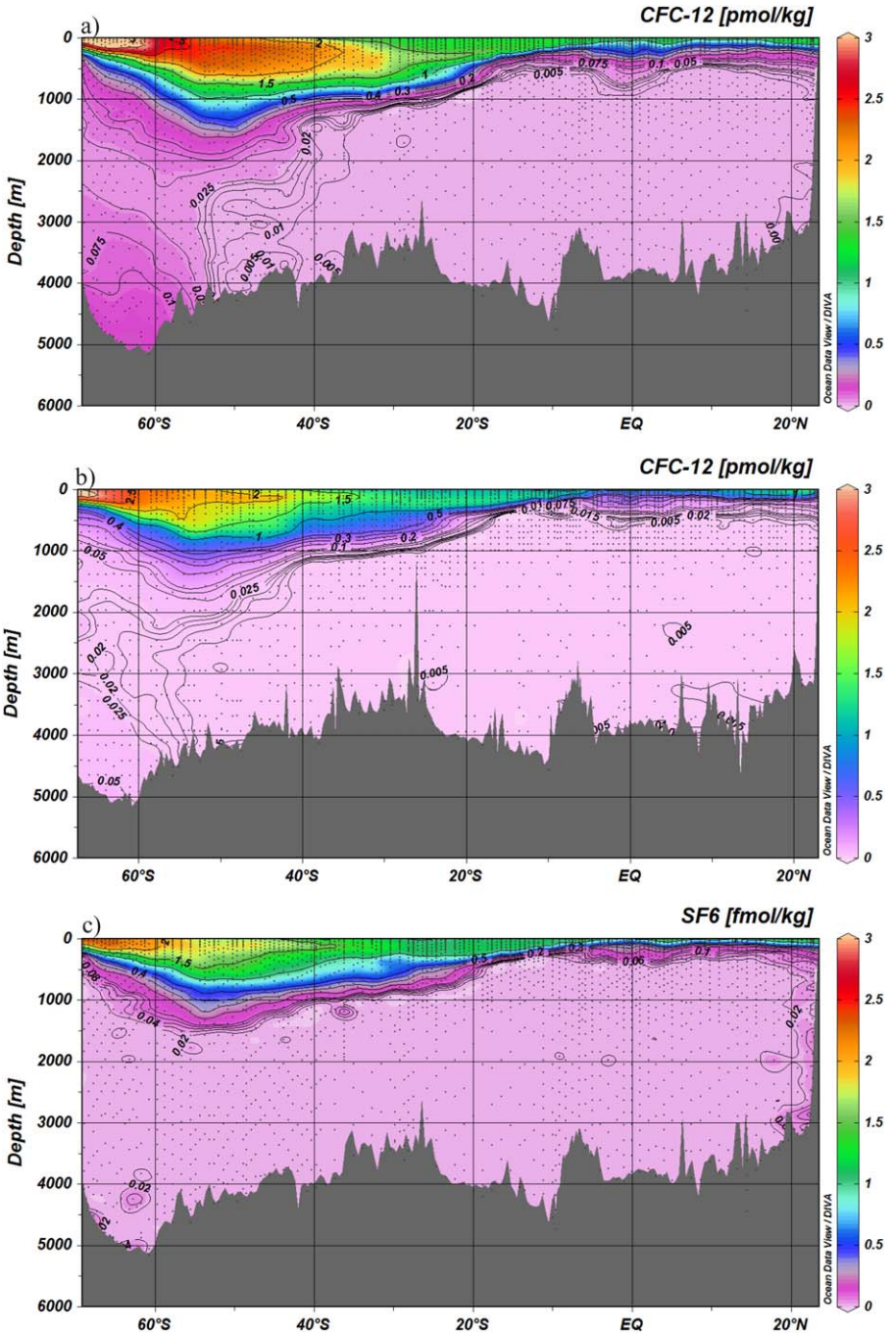

Figure 3. Concentrations of (a) CFC-12 in 2007/2008, (b) CFC-12 in 1994, both in pmol kg^{-1} (10^{-12} mol kg^{-1}), and (c) SF_6 in 2007/2008, in fmol kg^{-1} (10^{-15} mol kg^{-1}), measured along the P18 line in the Pacific Ocean. Dots indicate where water samples were collected.

3. Transit Time Distributions

To estimate mean ventilation timescales, TTDs were computed using the inverse Gaussian (IG) form that results from 1-D flow and mixing,

$$G(t) = \sqrt{\frac{\Gamma^3}{4\pi\Delta^2 t^3}}\ \exp\left[-\frac{\Gamma(t-\Gamma)^2}{4\Delta^2 t}\right] \quad (1)$$

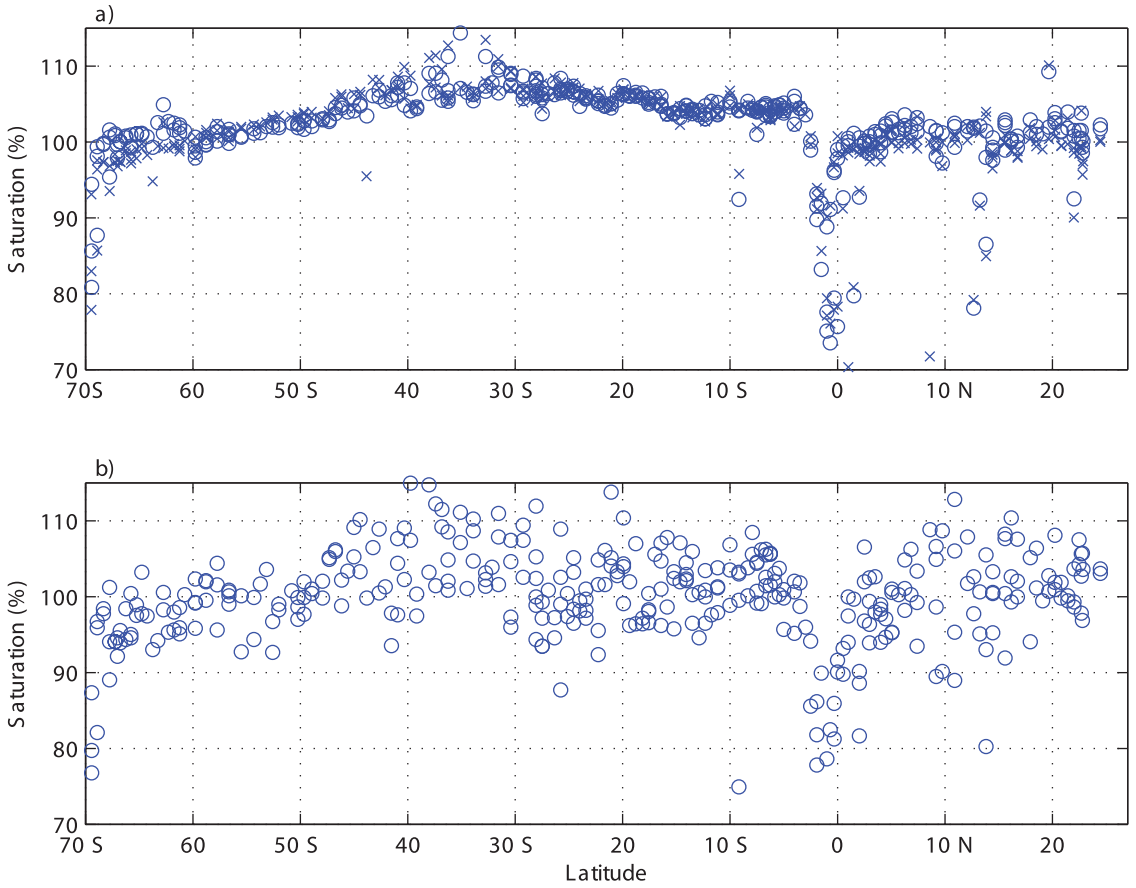

Figure 4. The percent saturation of (a) CFC-12 (o) and CFC-11 (x) and (b) SF_6 in surface water samples (depth $<$ 50m) measured relative to equilibration with respect to their hemispheric average concentrations in the atmosphere during 2007/2008.

where Γ and Δ are the first and second centered moments of the TTD, interpreted as the mean and width of the TTD [*Khatiwala et al*., 2001; *Waugh et al*., 2003]. Γ and Δ can be related to 1-D flow and mixing via the Peclet Number $Pe=(\Gamma/\Delta)^2$ [*Waugh and Hall*, 2002], where $Pe=vL/K$, and v and K are along streamline flow and mixing, respectively, and L is the transport length scale. A significant advantage of the IG functional form is that it can be fully described by two parameters, Γ and Δ. As pioneered by *Hall et al*. [2002] and *Waugh et al*. [2002, 2003, 2004], two transient tracers with independent time histories can in principle be used to fully constrain the IG TTD in the ocean interior.

Three-dimensional ocean model simulations indicate that in many oceanic regions and depth ranges, the TTD resulting from 3-D flow and mixing can be reasonably approximated by the simpler IG form (equation (1)). The IG form has been shown to fairly approximate 3-D transport in the subtropical North Atlantic [*Khatiwala et al*., 2001; *Haine and Hall*, 2002], and in the subtropical gyres in general [*Peacock and Maltrud*, 2006; *Sonnerup et al*., 2013], reflecting the fact that the dominant ventilation processes in the main subtropical thermocline are, to first order, primarily along isopycnals. However, significant differences between 3-D TTDs and the IG form were found in

Table 1. Sea Surface Saturation Levels Estimated for the Latitude Band and Mixed Layer Depth of the Climatological Wintertime Outcrop of Potential Density Layers along 105°W[a]

		Saturation Level (%)		
Density Range	Latitude Band	CFC-12	CFC-11	SF_6
$\sigma_\theta < 26.8$	40–45°S	100	102	100
$26.8 <= \sigma_\theta < 26.9$	46–50°S	97.5	100	97.5
$26.9 <= \sigma_\theta < 27.0$	50–55°S	95	97.5	95
$27.0 <= \sigma_\theta < 27.1$	55–58°S	90	90	90
$27.1 <= \sigma_\theta < 27.2$	58–61°S	88	88	85
$\sigma_\theta >= 27.2$	61–64°S	75	75	68

[a]These values were used for determining pCFC and pSF_6 ages and for calculating the tracer concentrations corresponding to the TTDs.

the Southern Ocean and equatorial regions, and indicated that equation (1) is likely only representative of TTDs that occur in the Southeast Pacific Ocean south of 30°S [*Peacock and Maltrud*, 2006; *Sonnerup et al*., 2013] and north of the Subantarctic Front (~ 57°S).

Because the atmospheric CFC histories since the 1990s no longer follow a quasi-exponential increase (Figure 1), a lookup table approach [*Stanley et al*., 2012] was used to find IG TTDs that concurrently satisfy the constraints provided by the pCFC-11, pCFC-12, and pSF_6 tracer concentrations. The lookup table consists of tracer partial pressures computed for a wide range and large number ($n \sim 2x10^5$) of IG TTDs, discretized uniformly from a minimum Γ of 6 months (~ the time elapsed since austral winter until P18 in austral summer, December 2007 to February 2008) up to 1000 years in increments of 0.25 years. For each Γ, Δ/Γ ratios from 0.1 to 5, in 0.1 increments, were considered. This range spans the IG TTDs that were consistent, in prior studies, with CFC/SF_6 measurements in the eastern subtropical and subpolar North Pacific Ocean [*Sonnerup et al*., 2013], and with CFCs and ^{3}H-^{3}He measurements in the North Atlantic Ocean [*Waugh et al*., 2004; *Stanley et al*., 2012]. Uncertainties in air-sea saturation state and analytical precision were included in confidence intervals used for matching tracer concentrations with the TTDs. For each P18 water sample, all IG TTDs from our table whose computed tracer values agreed within 1 σ confidence intervals with the observed pCFC-11, pCFC-12 and pSF_6 were identified. A match within 1 σ confidence intervals to all three tracer concentrations was found for ~ $^1/_2$ of the P18 samples and, for comparison, for ~ $^3/_4$ of the samples when 2 σ confidence intervals were used instead.

4. Results—P18 Tracer Measurements

The 2007/2008 CFC sections, compared with those collected in 1994, reflect the continued downward penetration of these compounds through the thermocline and into the abyssal Southern Ocean (Figure 3). In midlatitudes (20–40°S), although CFC levels in the upper 600 m were higher in 2007/2008, measureable CFCs, using a common definition of 0.005 pmol kg^{-1}, had not penetrated much deeper than in 1994. In the tropics, however, CFCs had penetrated to ~ 900 m in 2007/2008, as compared with ~650 m in 1994. The greatest differences were found south of 45°S, where CFCs (> 0.005 pmol kg^{-1}) penetrated to the sea floor as far north as 55°S in 1994, and as far north as 43°S in 2007/2008. The subsurface CFC concentration maximum at the sea floor south of 60°S, where CFC-12 levels were as high as 0.05 pmol kg^{-1} in 1994, exhibited levels higher than 0.1 pmol kg^{-1} over the bottom km everywhere south of 57°S in 2007/2008.

The atmospheric concentration histories of CFC-12 over the 40 year period preceding 1994, and SF_6 over the 40 year period preceding 2007/2008, have nearly identical relative trends (Figure 1). This coincidence is reflected in the similar depth distributions of CFC-12 during 1990s WOCE sections and SF_6 during recent (2000s) CLIVAR/RH sections (Figure 3) [*Tanhua et al*., 2013]. However, CFC-12 had, in 1994, penetrated to measurable levels deeper than SF_6 in 2007/2008, especially in the Southern Ocean (south of 50°S), where CFCs were everywhere detectable to the bottom in 1994. In contrast, SF_6 was only measurable (excepting a few isolated samples near the bottom) to ~ 1600 m in 2007/2008. This difference likely does not reflect a slowdown in abyssal ventilation in 2007/2008 as compared to 1994, but rather reflects both the lower atmospheric SF_6 concentrations (~ 100 times lower than CFC-12) and lower solubility of SF_6 in seawater [*Bullister et al*., 2002] precluding detection of this compound, highlighting the analytical challenge that dissolved SF_6 measurements present in comparison to the CFCs [*Bullister and Wisegarver*, 2008].

5. Results—Transit Time Distributions

In water samples from the subtropical and subantarctic Southeast Pacific Ocean, the Δ/Γ of TTDs of water samples matching the CFCs and SF_6 were usually on the order of 0.5–1.5 (Figure 5). In about $^3/_4$ of the shallower samples ($\sigma_\theta < 26.9$) and $^3/_5$ of all samples, the mean Δ/Γ of TTDs matching the tracer concentrations was less than 1. South of 45°S (Figure 5b), $\Delta/\Gamma > 2$ were common for water samples whose $\sigma_\theta > 26.9$ (note that $\Delta/\Gamma = 5$ was the maximum considered in the lookup table). In the subtropical gyre (45°S to 30°S, $\sigma_\theta < 26.9$), the CFC/SF_6 tracer combination was usually consistent with IG TTDs whose $\Delta/\Gamma < 1$.

The added constraint that SF_6 provides was evaluated by comparing the results from matching the tracer observations to the TTDs derived using CFC-11 and CFC-12 as constraints, and with those derived using just one CFC and SF_6. Use of just one CFC (CFC-11 or CFC-12) in conjunction with SF_6 provided results

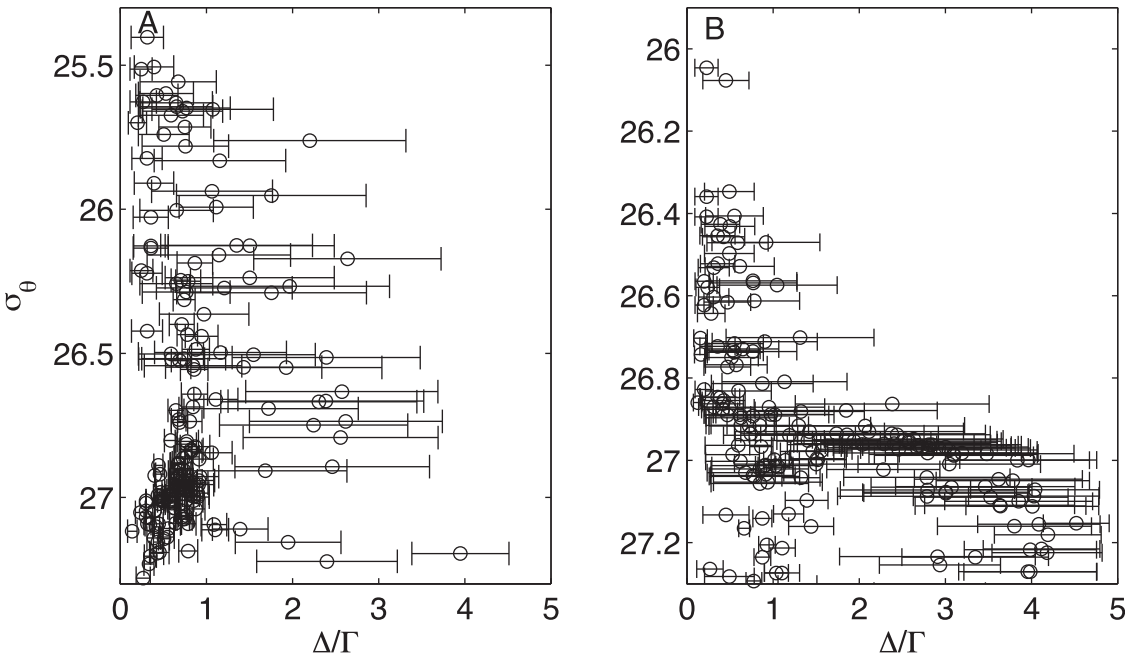

Figure 5. The mean and standard deviation of the Δ/Γ of the population of TTDs from the lookup table that matched water samples' partial pressures of CFC-11, CFC-12, and SF_6 during the 2007/2008 CLIVAR/RH P18 cruise in the South Pacific Ocean (a) from 30°S to 45°S and (b) from south of 45°S.

comparable to use of three tracers: both CFC-11 and CFC-12 with SF_6. The use of the CFC pair alone generally indicated higher relative mixing (higher Δ/Γ), with the values of Δ/Γ being approximately 1 for potential densities less than 26.6 σ_θ, and $\Delta/\Gamma >> 1$ deeper than 26.8 σ_θ. The inclusion of SF_6 thus provided additional time information that tightened constraints on mixing's effects on the tracer ages [*Waugh et al.*, 2002, 2003], and generally indicated lower Δ/Γ in the IG TTDs from this data set.

An additional constraint on the TTDs was available from the fact that CLIVAR/RH P18 line is a repeat of the 1994 WOCE P18 line. Assuming that the overall rate of organic matter cycling has not changed, the possibility of ventilation changes was evaluated from the changes in apparent oxygen utilization ($AOU = O_{2\ saturation} - O_{2\ measured}$) observed between 1994 and the 2007/2008 reoccupation (Figure 6). From 1994 to 2007/2008, south of 42°S to 55°S there was an increase in AOU from 500 to 1000 m, consistent with a slowdown in

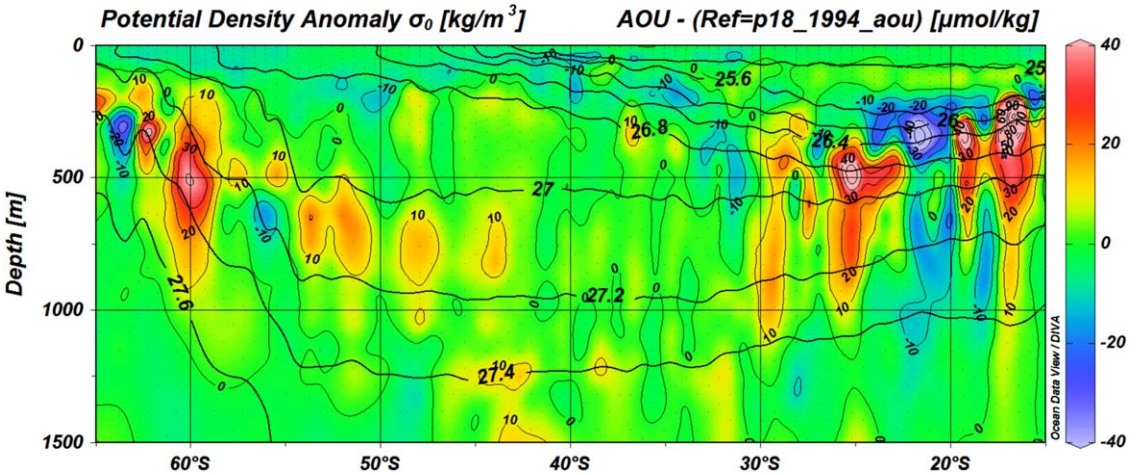

Figure 6. The differences in AOU between the 2007/2008 CLIVAR/RH and the 1994 WOCE P18 cruises, defined as 2007/2008 AOU minus 1994 AOU, in μmol kg^{-1}, with 2007/2008 potential density contours overlain.

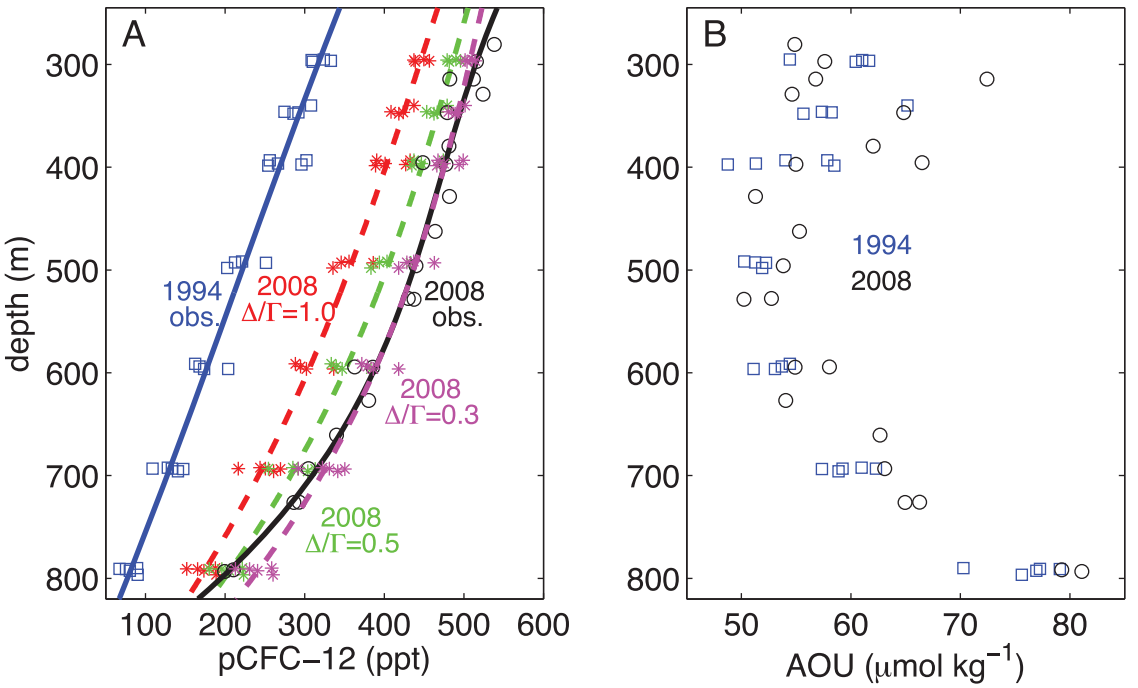

Figure 7. (a) The 1994 (blue squares) and 2007/2008 (black circles) pCFC-12 measured from 33° to 37°S along the P18 line, ~ 103°W in the South Pacific Ocean. IG TTDs fit to the 1994 pCFC-12 were used to forecast the 2007/2008 pCFC-12 that would occur under steady transport, using $\Delta/\Gamma = 1$ (red stars), 0.5 (green stars), and 0.3 (magenta stars) assuming uniform 10% undersaturation at the sea surface [*Waugh et al.*, 2013]. Solid and dashed lines are polynomials fit through the data and TTD predictions, respectively. The best fit to $\Delta/\Gamma = 0.3$ was obtained whether full (100%) or reduced (90%) sea surface saturation, or those estimated in 1994 [*Sonnerup et al.*, 1999b] or in 2007/2008 (Table 1) were used. (b) The 1994 (blue squares) and 2007/2008 (black circles) AOU measured from 33° to 37°S along the P18 line, ~ 103°W in the South Pacific Ocean. The latitude band 33–37°S matches that presented in *Tanhua et al.* [2013], however the changes in AOU and TTDs whose $\Delta/\Gamma = 0.3$ were consistent with steady transport throughout the region 30–42°S, depth < 800 m.

ventilation also noted from changes in CFCs [*Waugh et al.*, 2013]. This feature persists when the CLIVAR/RH and WOCE AOU fields are gridded and subtracted versus potential density instead of depth. However, in the subtropics the 2007/2008 and 1994 AOU comparison indicated no appreciable change from 30° to 42°S (< 800 m) that, assuming that biological oxygen consumption rates in the region have not changed, indicated that the ventilation in this portion of the Southeast Subtropical Pacific had not changed appreciably since WOCE (Figure 6). In this region, then, the pCFC increase from 1994 to 2007/2008 was used to estimate the Δ/Γ of the IG TTDs [*Waugh et al.*, 2003].

The *Waugh et al.* [2003, 2013] and *Tanhua et al.* [2013] methodology was followed in detail for the depth range 200–800 m, 30° to 42°S. Based on the lack of change in AOU (Figure 6), it was assumed that the ventilation has remained steady in this region. TTDs (from the lookup table) were selected that matched the 1994 WOCE pCFC-12 observations. The pCFC-12 forecasted for 2007/2008 by these TTDs were then compared with the pCFC-12 observed during CLIVAR/RH. In this depth and latitude range, the decadal pCFC-12 increase predicted by any TTD with $\Delta/\Gamma > 0.5$ was smaller than the observed increase (Figure 7a) [*Tanhua et al.*, 2013]. If values of $\Delta/\Gamma > 0.5$ were chosen to fit the 1994 P18 CFC data, then the 1994–2007/2008 pCFC-12 increase could be interpreted to indicate that the ventilation in this region had accelerated during 1994–2007/2008. With steady transport, a best fit to both the 1994 and 2007/2008 pCFC data was obtained with IG TTDs whose $\Delta/\Gamma = 0.3$ (Figure 7a) throughout the region 30° to 42°S, < 800 m. This value is not inconsistent with the 2007/2008 CFC and SF_6 tracer suite (Figure 5a), indicating that both the steady AOU (Figure 7b) and the 1994 to 2007/2008 increase in pCFC-12 observed are consistent with steady ventilation in this region. Apparently the higher Δ/Γ TTDs (> 0.5), and the coarse (2°) resolution 3-D models used in *Waugh et al.* [2013] and in *Tanhua et al.* [2013] mixed away part of 1994–2007/2008 pCFC increase in the subtropics along 103°W.

In the upper 800 m of the subtropics, the high Peclet number (low Δ/Γ) flow characteristics consistent with the 1994–2007/2008 pCFC increase and the 2007/2008 pSF_6/pCFC tracer combination would indicate that

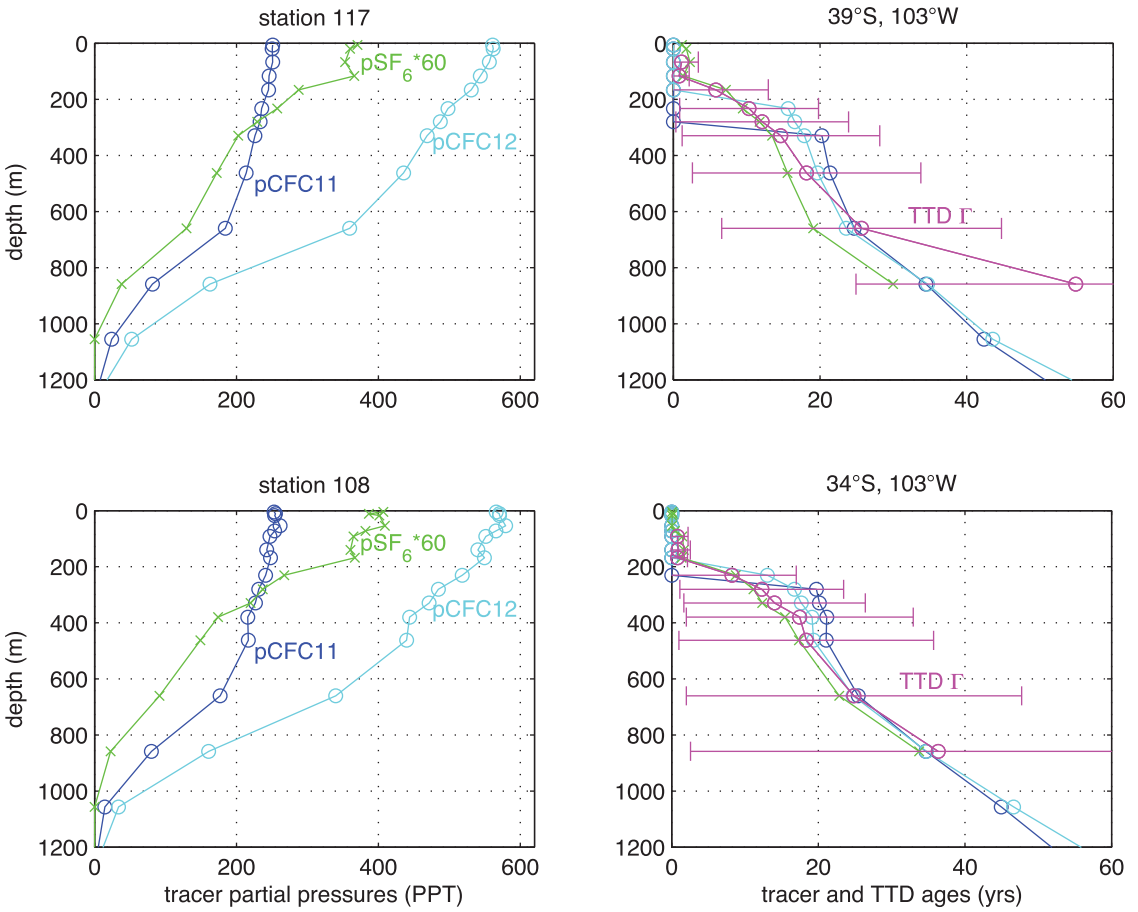

Figure 8. (left) The partial pressures for CFC-11 (blue), CFC-12 (cyan), and SF_6 (green), and (right) partial pressure and TTD mean ages (magenta) calculated from the pCFC and pSF_6 measured at station (top) 117 and (bottom) 108 along the 2007/2008 CLIVAR/RH P18 line. Uncertainties in the tracer ages are omitted for clarity and were usually smaller than the symbols. Uncertainties in the TTD mean ages reflect the scatter in the population of TTDs from the lookup table that matched the tracer partial pressures for each sample.

the tracer ages are relatively unaffected by mixing. Indeed, in samples with detectable SF_6, the tracer ages usually agreed reasonably well with the mean ages (Γ) implied by the TTDs in this region (Figure 8). Near the sea surface ($<$ 400 m), Γ were usually coincident with tracer ages determined from pSF_6 alone. These water mass ages were $<$ 15 years, indicating that the water samples were mostly derived from components that outcropped during the post-1990 linear portion of the atmospheric SF_6 history (Figure 1). As outlined in *Waugh et al.* [2003], tracers with linear growth/decay histories will yield tracer ages = Γ. Similarly, from 500 to 700 m, and often deeper, the pCFC ages were in agreement with Γ (Figure 8). These samples would have, on average, outcropped during the 1970s and 1980s, the linear window of CFC growth in the atmosphere (Figure 1). Within the subtropical South Pacific thermocline along 103°W, then, pSF_6 ages corresponding to vintages after $\sim$ 1990, and pCFC ages corresponding to vintages in the 1970s and 1980s, may be used as a simpler substitute for Γ. The measured tracer concentrations were usually consistent with a wide range of Γ, however (Figure 8).

Outside of the subtropics, the tracer ages differed from TTD mean ages (Figure 9). South of 45°S, the Γ were systematically $<$ pSF_6 ages in the upper $\sim$450 m, although they agreed within uncertainties in measurements and SF_6 sea surface saturation state. The CFC levels in these samples tended to be very near saturation, decreasing the average Γ of matching TTDs, that then had significant implications in these shallow samples for the estimated oxygen utilization rates (discussed below). South of 45°S, Γ were always $>$ pCFC (and pSF_6) ages for pCFC ages $>$ 30 years in 2007/2008. The fact that mixing has impacted the tracer ages, biasing pCFC and pSF_6 ages younger than mean ages, was evident from the systematic offset between pCFC and pSF_6 ages of greater than 5 years. North of 30°S along this section the situation was similar: pSF_6

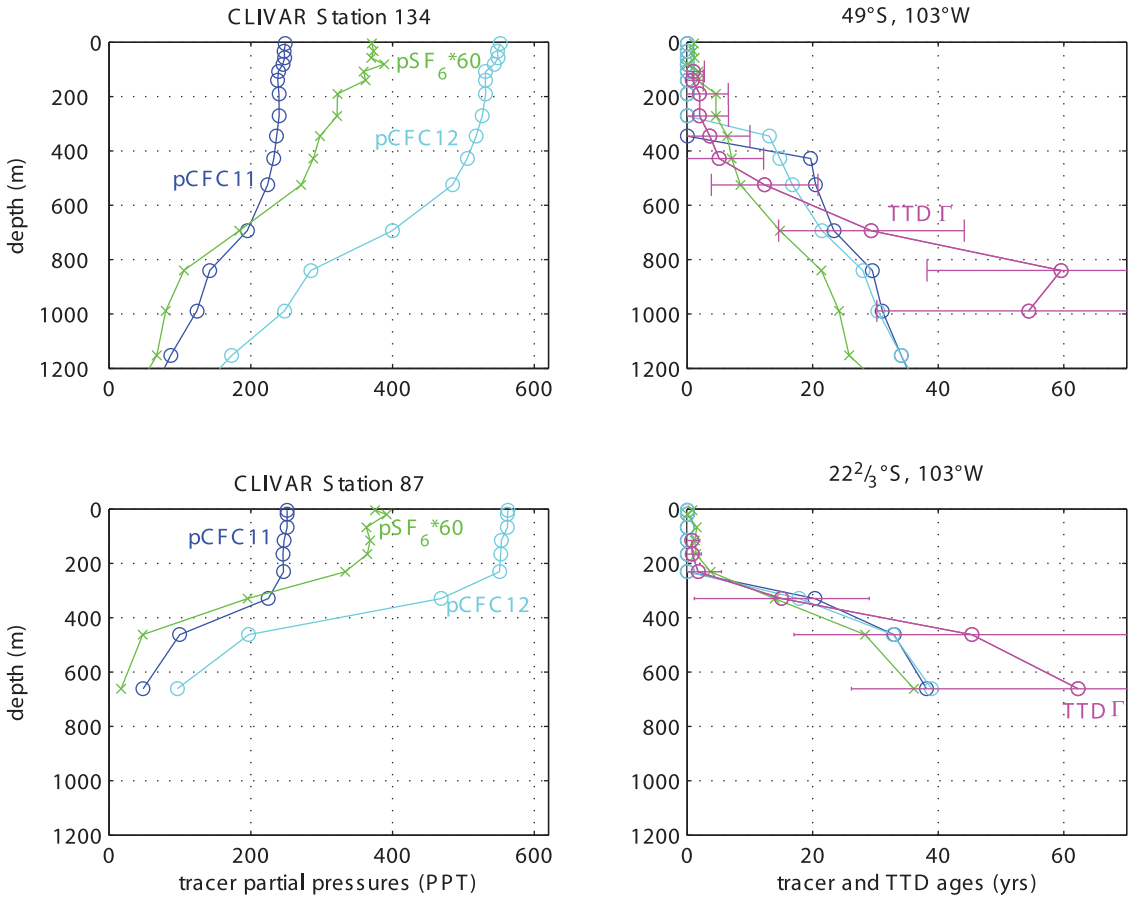

Figure 9. (left) The tracer partial pressures, and (right) partial pressure and TTD mean ages calculated from the pCFC and pSF_6 measured at station (top) 134 and (bottom) 87 along the 2007/2008 CLIVAR/RH P18 line, and color coded as in Figure 8.

and pCFC ages agreed with Γ for pSF_6 and pCFC ages < 30 years, but were usually $\sim$ twofold younger than Γ in samples deeper (older) than that age (Figure 9).

6. Oxygen Utilization Rates—OURs

6.1. In Situ OUR From Isopycnal Gradients in AOU and Γ (OUR_{grad})

The mean transit timescales from the TTDs were used to estimate oxygen utilization rates, as they represent the time scale over which the AOU observed at depth has accumulated, and provide an estimate of the impacts that mixing has on the individual tracer (pCFC or pSF_6) ages. Although the tracer partial pressure ages and the TTD mean ages are comparable over a significant portion of our study area, we utilized the TTD mean age timescales, Γ, here, as they can be significantly different at depth, and both Γ and AOU represent a quasi-steady state field. We confined our analysis to south of 30°S where both model simulations [*Peacock and Maltrud*, 2006; *Sonnerup et al.*, 2013] and the success of the TTD lookup table in matching the measured tracers, indicated the IG form (equation (1)) to be applicable. It was assumed that isopycnal transport dominates over diapycnal [*Jenkins*, 1987], and that isopycnal trends in Γ and AOU are thus due to ageing and concomitant oxygen consumption. The OUR were estimated from isopycnal gradients in AOU and ventilation age:

$$OUR_{grad} = \frac{\nabla AOU}{\nabla \Gamma} \tag{2}$$

where $\bigtriangledown$ *AOU* and $\bigtriangledown\Gamma$ represent spatial gradients in AOU and in Γ, respectively [*Warner et al.*, 1996]. The observations were binned into isopycnal horizons, and for each horizon OUR_{grad} was computed from the AOU versus Γ trend [*Jenkins*, 1987; *Warner et al.*, 1996] in two regions, 30°S to 42°S, and 43°S to 54°S. This

Table 2. Oxygen Utilization Rates From Isopycnal Trends in AOU and the Mean Transit Time (Γ) of TTDs That Match the SF_6 and CFC Observations From 30° to 42°S Along 103°W in the Eastern Subtropical South Pacific Ocean[a]

Density Range (σ_θ)	Depth Range (m)	Latitude Band	O.U.R. (μmol kg^{-1} yr^{-1})	N
25.5–26.0	120–230	30°–37°S	6.4 ± 1.5	16
26.0–26.5	120–320	30°–40°S	3.1 ± 0.4	18
26.5–26.8	170–380	30°–42°S	2.7 ± 0.2	17
26.8–26.9	250–430	30°–42°S	2.3 ± 0.2	13
26.9–27.0	320–560	30°–42°S	1.7 ± 0.3	24
27.0–27.1	590–790	30°–42°S	1.3 ± 0.2	23
27.1–27.2	830–960	30°-42°S	0.8 ± 0.4	8

[a]The depths are the range for all samples within the latitude band analyzed.

approach assumes that the isopycnal age (Γ) and AOU fields are oriented in parallel and, for a meridional section, that the gradients are primarily oriented north-south. For the Southeast Pacific Ocean (south of 30°S) along 103°W this was confirmed via isopycnal analysis of the WOCE-era CFC and O_2 data sets [i.e., *Sonnerup et al.*, 2007], assuming that pCFC-11 and pCFC-12 represent a proxy for age, Γ.

6.2. Path-Integrated OURs (OUR_{path})

Oxygen utilization rates were also estimated by dividing each water sample's AOU by the mean age, Γ, of the TTDs that match its tracer concentrations:

$$OUR_{path} = \frac{AOU}{\Gamma} \tag{3}$$

The apparent, or path integrated, OUR determined from this approach represents the average OUR over the pathways of the water parcels to the sample location in the ocean interior [*Jenkins*, 1987; *Doney and Bullister*, 1992], and not necessarily the OUR occurring at the sample location. In the lower thermocline, for example, OUR_{path} are likely higher than in situ (OUR_{grad}) because the AOU of these deeper samples reflects the integrated O_2 consumption that included that occurring in regions where the isopycnal shoals. Assuming that O_2 consumption rates attenuate with increasing depth [*Stanley et al.*, 2012; *Sonnerup et al.*, 2013], OURs estimated from (3) will be biased systematically high in the lower thermocline, and trends in the depth-integrated OUR will tend to be spatially smoothed. This bias does not occur in shallower samples ($<$ 300 m), where the bulk of O_2 consumption occurs, so the total O_2 consumption inferred from integration of a depth profile of OUR_{path} may not be biased significantly. Because the OUR_{path} approach requires less data—the measured temperature, salinity, dissolved oxygen, CFC, and SF_6 at a particular location, it can provide spatial trends in the depth-integrated OUR, and in implied organic carbon export rates, from the overlying sea surface.

7. OURs—Results

7.1. In situ OUR From Isopycnal Gradients in AOU and Γ (OUR_{grad})

The OUR_{grad} were estimated from isopycnal gradients in AOU and ventilation age (equation (2)). In the subtropics, the OUR_{grad} (Table 2) decreased with increasing density (depth) from $\sim$ 6.4 ± 1.5 μmol kg^{-1} yr^{-1} on 25.5–26.0 σ_θ ($\sim$120–230 m), to 0.8 ± 0.4 μmol kg^{-1} yr^{-1} on 27.1–27.2 σ_θ ($\sim$830–960 m). In the region 43°S to 54°S, the OUR_{grad} (Table 3) decreased with increasing density from 16.6 ± 2.7 μmol kg^{-1} yr^{-1} on 26.5–26.8 σ_θ ($\sim$120–190 m) to negligible rates (0.01 ± 0.01 μmol kg^{-1} yr^{-1}) on 27.1–27.2 σ_θ ($\sim$740–960 m). Denser (deeper) than 27.2 σ_θ ($\sim$ 1000 m) OUR_{grad} were indistinguishable from zero in both regions, due to the attenuation of OUR with increasing depth, and because low SF_6 in 2007/2008 precluded precise determination of Γ. Uncertainties in OUR_{grad} reflect the scatter in the isopycnal AOU versus Γ trends. Integrating the OUR_{grad} depth profiles (Tables 2 and 3) from 120 to 960 m, and converting into carbon units in the C:O_2 ratio of 1:1.45 [*Anderson and Sarmiento*, 1994], implied an average organic carbon (OC) remineralization rate in this depth range of 1.2 ± 0.1 moles C m^{-2} yr^{-1} in the subtropics, and 1.3 ± 0.1 moles C m^{-2} yr^{-1} from 43°S to 54°S. This depth integration likely places a lower bound on the total C remineralization as it misses the base of the euphotic zone where significant remineralization occurs [*Martin et al.*, 1987; *Kadko*, 2009]. However, these OURs represent an estimate of the oxygen consumption occurring in situ, and are useful for comparison to the path-integrated OUR determined below.

7.2. Path-Integrated OURs (OUR_{path})

In the subantarctic region (e.g., Station 134 at 49°S, Figure 10), OUR_{path} from TTDs attenuated rapidly from 10 to 15 μmol kg^{-1} yr^{-1} from 200 to 300 m to $\sim$ zero by 800 m. Where the depth ranges coincided, the

Table 3. Oxygen Utilization Rates Determined From Isopycnal Trends in AOU and the Mean Transit Time (Γ) of TTDs That Match the SF_6 and CFC Observations, From South of 43°S Along 103°W in the Eastern South Pacific Ocean[a]

Density range (σ_θ)	Depth range (m)	Latitude Band	O.U.R. (μmol kg^{-1} yr^{-1})	N
26.5–26.8	120–190	43°–47°S	16.6 ± 2.7	8
26.8–26.9	170–250	43°–50°S	4.3 ± 1.4	8
26.9–27.0	230–590	43°–50°S	1.0 ± 0.1	29
27.0–27.1	540–790	43°–54°S	0.8 ± 0.1	14
27.1–27.2	740–960	43°–54°S	0.01 ± 0.01	11

[a]The depths are the range for all samples within the latitude band analyzed.

OUR_{path} tended to be higher than OUR_{grad} (Table 3) in this region. From 200 to 400 m, OUR_{path} from TTDs tended to be higher than from pSF_6 because the Γ tuned to both CFCs and SF_6 were often younger than pSF_6 ages in this depth range and south of 45°S, as discussed above. In the subtropics (e.g., Stations 108 at 34°S, and 104 at 32°S, Figure 10), OUR_{path} from Γ near the base of the wintertime mixed layer (150–200 m) were approximately 12 μmol kg^{-1} yr^{-1}, attenuating to ~2.5 μmol kg^{-1} yr^{-1} by 400 m. OUR_{path} values were never lower than 2 μmol kg^{-1} yr^{-1} in the upper 800 m within the subtropics. OUR_{path} from Γ were usually significantly higher than OUR_{grad}, possibly reflecting the systematic bias due to path integration discussed above. In deeper samples (> 450 m), part of the discrepancy could be due to O_2 undersaturation during wintertime subduction, which would bias OUR_{path} and not OUR_{grad} to higher values. This 'preformed AOU' likely has only small effect in the shallow (< 450 m) samples where the discrepancy between OUR_{path} and OUR_{grad} is largest, however, as these shallow isopycnals ($\sigma_\theta < 26.9$) exhibited nearly full O_2 (and CFC, Table 1) saturation at their outcrop locations [*Hartin et al.*, 2011]. Uncertainties due to O_2 undersaturation during water mass formation (~8–11 μmol kg^{-1} in remnant winter mixed layers for $\sigma_\theta > 26.9$, i.e., Table 1) made only a small contribution to uncertainties in OUR_{path}, which resulted primarily from uncertainties in Γ (Figures 8 and 9). Deeper than ~800 m, SF_6 levels were too low in 2007/2008 to confidently assign TTDs in this region. From 300 to 800 m in the subtropics (30–45°S), OUR_{path} from tracer partial pressures (pSF_6 and pCFC ages) were comparable to those using TTD mean ages, Γ, as expected from the good agreement between the various tracer dating methods in this region and depth range (Figure 8). At some subtropical stations (e.g., Station 104 at 32°S, Figure 10), OUR_{path} at 150 m were lower than at 200 m. This minimum may reflect biological O_2 production in these waters that encounter appreciable light due to isopycnal heaving [*Letelier et al.*, 2004; *Nicholson et al.*, 2008]. Indeed, dissolved oxygen isotopic measurements indicate biological production occurring in this depth range along the P18 section from 30 to 50°S (L. Juranek, personal communication, 2013).

The OUR_{path} profiles from Γ (Figure 10) at individual stations were depth-integrated to estimate organic carbon export rates from the overlying sea surface, as reflected in the AOU of the underlying thermocline. For example, the OUR_{path} at 49°S, 103°W (Station 134, Figure 10), can be depth-integrated (200 m to 850 m) and converted to C-units as above, to estimate an OC remineralization rate of 2.4 ± 0.4 mol C m^{-2} yr^{-1}.

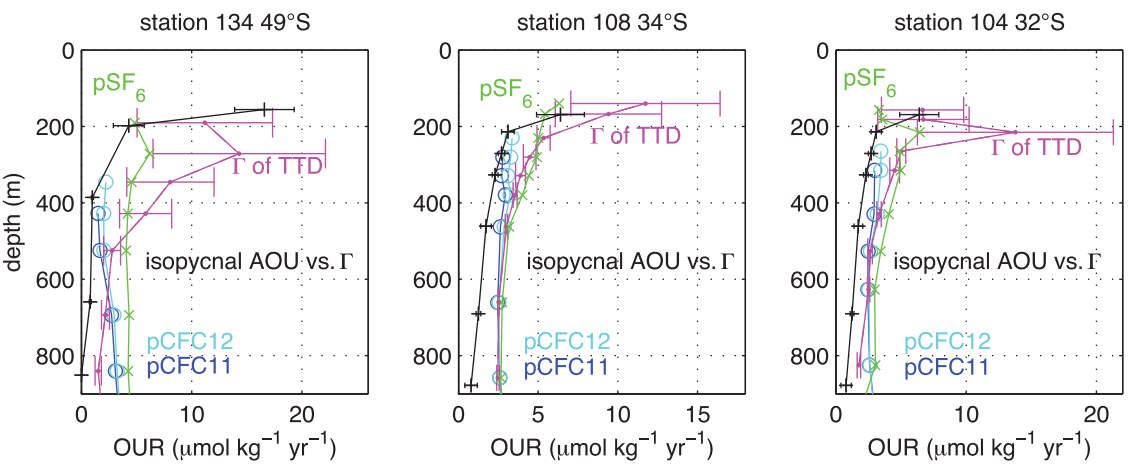

Figure 10. Depth profiles of OUR_{path} from AOU divided by tracer ages from pCFC-11 (blue), pCFC-12 (cyan), pSF_6 (green), and by the mean Γ of TTDs matching all three tracers (magenta) in discrete samples at stations (left) 134, (middle) 108, and (right) 104 during the 2007/2008 CLIVAR/RH P18 line. OUR_{grad} (equation (2)) from corresponding regions (Tables 2 and 3) are included for comparison (black). Error bars on the pSF_6 age and pCFC age derived OUR_{path} are omitted for clarity, and were comparable to the symbol sizes.

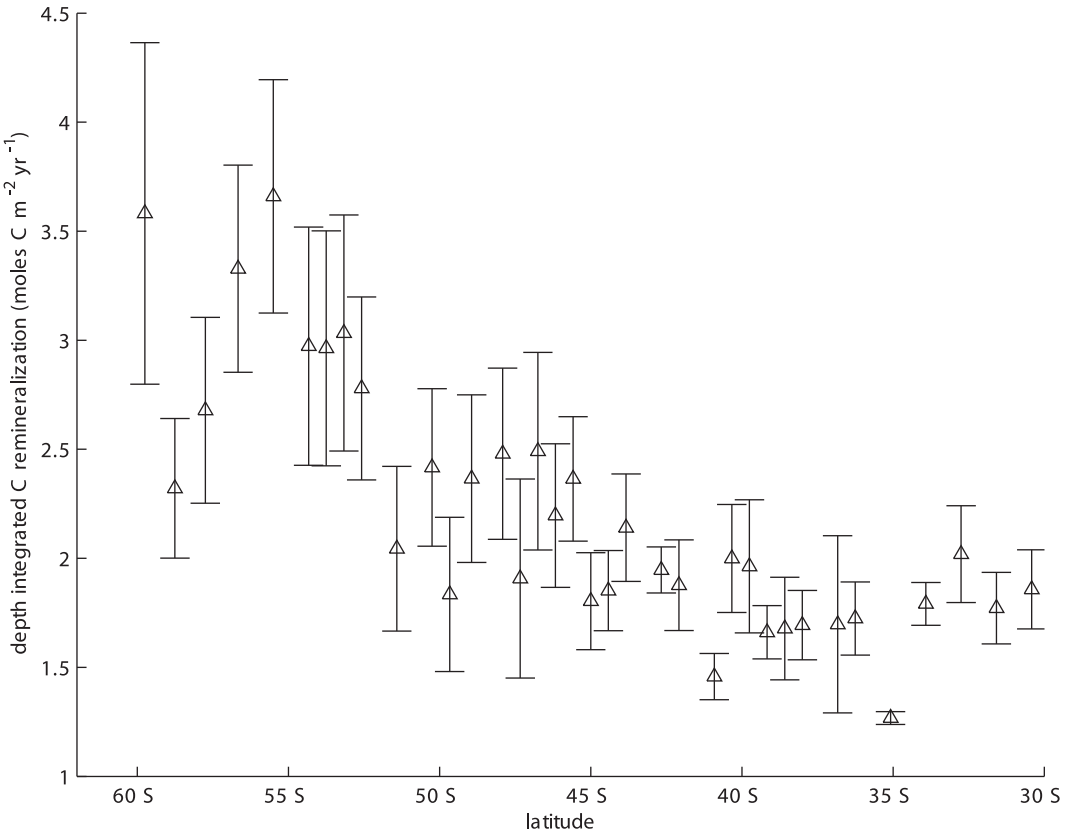

Figure 11. The meridional trend in OC export inferred from the depth-integrated OUR_{path} (equation (3)), from stations occupied during the 2007/2008 CLIVAR/RH P18 line along 103°W in the South Pacific Ocean.

This was higher than at subtropical stations where, for example, integrating the OUR_{path} depth profiles from 34°S and 32°S (Figure 10) from 150 m down to 800 m implied total C-remineralization rates on the order of 1.8 ± 0.2 moles C m^{-2} yr^{-1} (Figure 11). Overall, in the Southeast Pacific Ocean along the P18 line, depth-integrated OUR_{path} converted to C units were on the order of ~1.8 moles C m^{-2} yr^{-1} from 30°S to 45°S, 2–2.5 moles C m^{-2} yr^{-1} from 45°S to 52°S, and 2.5–3.5 moles C m^{-2} yr^{-1} from 52°S to 60°S (Figure 11).

8. Summary and Discussion

The procedure of tuning the IG TTD form to the readily available tracer suite—CFC-11, CFC-12, and SF_6 was evaluated. Inclusion of SF_6 usually indicated lower relative rates of mixing, $\Delta/\Gamma < 1$, than did the use of CFCs alone. Although the CLIVAR/RH CFC/SF_6 tracer data set was usually consistent with prior findings [*Waugh et al.*, 2004] that $\Delta/\Gamma = 1$ fit the tracers well, in about ¾ of samples from $\sigma_\theta = 26.9$ and shallower along the P18 line, Δ/Γ was often < 1 using the SF_6/CFC tracer combination. The 1994–2007/2008 increase in pCFC-12 in the subtropics (30–42°S, 200–800 m), where ventilation was presumed to have been steady due to near-zero changes in AOU, indicated $\Delta/\Gamma \sim 0.3$, consistent with the pSF_6/pCFC tracer suite in 2007/2008. Using CLIVAR/RH P6 data from along 32°S in the Pacific Ocean, *Kim et al.* [2013] found that IG TTDs with a Δ/Γ ratio on the order of 0.6 were maximally consistent with CFC-12, CFC-11 and SF_6 in 2009/2010. Their results, focused on the oxygen minimum layer (1100–2000 m), are consistent with the Δ/Γ ratios inferred here for individual samples using the same tracer suite. It may be that the low Δ/Γ indicated in the subtropics along P18 reflect the fact that these waters are fairly homogeneous and directly ventilated from the south, so mixing within these waters would be difficult to detect with the tracers available.

One implication of the low Δ/Γ TTDs is that the tracer ages are relatively unaffected by mixing, and are comparable to each other and to the mean transport timescale Γ of the TTD. This means that the tracer ages yield ventilation/overturning timescales relatively unbiased by mixing and may be confidently applied,

as a simpler substitute for Γ, to estimate anthropogenic CO_2 uptake, in situ oxygen consumption, and nutrient cycling rates over most of the subtropical thermocline along 105°W in 2007/2008. The depth range over which this simpler strategy may be employed will evolve with the passage of time as these tracers penetrate downward into the ocean interior [*Mecking et al*., 2004, 2006; *Sonnerup et al*., 2008]. As suggested by 3-D modeling studies in the subtropical North Atlantic [*Haine and Hall*, 2002], and from tracer measurements along 152°W in the subtropical North Pacific [*Sonnerup et al*., 2013], the IG form is consistent with the CLIVAR/RH CFC/SF_6 tracers, and possibly with the oceanic TTD, in this meridional section located downstream of a major mode water formation region.

Outside of the subtropics, however, the tracer ages differ from TTD mean ages. This situation is often, but not always, easily diagnosed from significant differences among the tracer ages (Figure 9) [*Sonnerup*, 2001]. North of 30°S along 103°W, IG TTDs matched the CFC-SF_6 tracer suite in only $\sim^1/_3$ of the samples collected. The fact that the IG form is often not consistent with the tracer observations may indicate that the IG form does not accurately represent the oceanic TTD in this region, as shown before in 3-D models [*Peacock and Maltrud*, 2006]. Relaxing the criterion used when matching the TTDs to the measurements from 1σ to 2σ improved the situation somewhat: TTDs matched the tracers north of 30°S, and over the whole section, for $> ^3/_4$ of the samples. Relaxing the matching criterion changes the properties of the IG TTDs inferred, however, increasing the Δ/Γ of the TTDs ultimately to 2.5, the mean Δ/Γ of the TTDs considered in the lookup table. The lower Δ/Γ indicated here, as compared with in prior studies [*Waugh et al*., 2004; *Stanley et al*., 2012; *Sonnerup et al*., 2013], may thus be due, at least in part, to the tighter precisions obtained in the CLIVAR/RH P18 CFC and SF_6 measurements than in prior data sets.

Along the P18 line, the depth-integrated OUR_{path} determined from TTDs and the AOU field indicated OC export rates from the mixed layer on the order of ~1.8 moles C m^{-2} yr^{-1} from 30°S to 45°S, 2–2.5 moles C m^{-2} yr^{-1} from 45°S to 52°S, and 2.5–3.5 moles C m^{-2} yr^{-1} from 52°S to 60°S (Figure 11). Depth integration of the OUR_{path} as a means to determine OC export is difficult to validate locally, due to a lack of organic carbon export rate determinations from the Southeast Pacific Ocean. Where such comparisons have been possible, such as the Northeast Pacific Ocean, the depth-integrated OUR_{path} from tracers [*Sonnerup et al*., 1999a, 2013] have shown good agreement with OC export estimated variously from mixed layer C, ^{13}C, O_2/Ar, and sediment trap fluxes [*Benitez-Nelson et al*., 2001; *Brix et al*., 2006; *Quay and Stutsman*, 2003; *Emerson et al*., 2008; *Emerson and Stump*, 2010]. The depth-integrated OUR_{path} from the Southeast Pacific (Figure 11) were smaller than in the Subtropical North Pacific at corresponding latitudes. In the Northeast Pacific (152°W) from 30° to 40°N, for example, depth-integrated OUR_{path} were 2.5–4 moles C m^{-2} yr^{-1} [*Sonnerup et al*., 2013], larger than along 103°W in the South Pacific, 1.5–2 moles C m^{-2} yr^{-1} (Figure 11). Although there are few OC export rate estimates to compare with depth-integrated OUR_{path} in this region, OC export rates on the order of ~ 2 moles C m^{-2} yr^{-1} estimated in the Subantarctic Zone (40–50°S), and of ~ 4 moles C m^{-2} yr^{-1} in the Polar Frontal Zone (50–60°S) in the Southwest Pacific Ocean (~ 180°E) estimated from mixed-layer O_2/Ar budgets [*Reuer et al*., 2007] agree well with the depth-integrated OUR_{path} along 103°W.

The depth-integrated OUR_{path} (Figure 11) were in excellent agreement with those based on inverse models of the marine tracer and nutrient/O_2 fields in the subtropics (1.7 to 2.9 moles C m^{-2} yr^{-1}), and were a bit higher than the inverse-model results south of 50°S (1.7–3.3 moles C m^{-2} yr^{-1}) [*Schlitzer*, 2002]. Satellite ocean color imagery, used to estimate chlorophyll concentrations, would indicate much lower productivity in the Southeast versus Northeast Pacific subtropical gyres [e.g., *Behrenfeld and Falkowski*, 1997]. Compared with satellite algorithms, even if the *Laws et al*. [2000] temperature dependence of export production is used, the depth integrated OUR_{path}, and depth integrated OUR_{grad}, and inverse-model results [*Schlitzer*, 2002] indicate significantly higher OC export rates in this region, and in particular south of 50°S. As noted by *Schlitzer* [2002], it appears that the AOU of subsurface waters, coupled with the oxygen supply rate provided by ventilation as estimated with tracer concentrations, are not consistent with the low rates of productivity indicated by satellite chlorophyll in this region of the South Pacific Ocean.

Acknowledgements

R. Sonnerup was supported by NSF grant OCE-0762517 and NOAA grant GCC NA10OAR4310090. S. Mecking was supported by NOAA grant NA11OAR4310064 and by NSF grant OCE-1059886. J. Bullister was supported by the NOAA Climate Observation Division. M. Warner was supported by NSF grants OCE-0762517 and OCE-0752980. We thank D. Wisegarver and the many participants on the P18 cruises for the high quality data collected. Two anonymous reviewers greatly improved the manuscript. This is JISAO contribution 2412 and PMEL contribution 4287. The P18 CFC and SF_6 data from 1994 and 2007/2008 are available at the CLIVAR and Carbon Hydrographic Data Office (http://cchdo.ucsd.edu).

References

Anderson, L. A., and J. L. Sarmiento (1994), Redfield ratios of remineralization determined by nutrient data analysis, *Global Biogeochem. Cycles*, *8*(1), 65–80.

Behrenfeld, M. J., and P. G. Falkowski (1997), Photosynthetic rates derived from satellite-based chlorophyll concentration, *Limnol. Oceanogr.*, *42*, 1–20.

Benitez-Nelson, C., K. O. Buesseler, D. M. Karl, and J. Andrews (2001), A time-series study of particulate matter export in the North Pacific Subtropical Gyre based on ^{234}Th:^{238}U disequilibrium, *Deep Sea Res., Part I*, *48*, 2595–2611.

Brix, H., N. Gruber, D. M. Karl, and N. R. Bates (2006), On the relationships between primary, net community, and export production in the subtropical gyres, *Deep Sea Res., Part II*, *53*, 698–717.

Bullister, J. L. (1989), Chlorofluorocarbons as time dependent tracers in the ocean, *Oceanogr. Mag.*, *2*, 12–17.

Bullister, J. L. (2015), Atmospheric Histories (1765–2015) for CFC-11, CFC-12, CFC-113, CCl_4, SF_6 and N_2O, *NDP-095*. Carbon Dioxide Inf. Anal. Cent., Oak Ridge Natl. Lab., US Dep. of Energy, Oak Ridge, Tenn, doi:10.3334/CDIAC/otg.CFC_ATM_Hist_2015. [Available at http://cdiac.ornl.gov/ftp/oceans/CFC_ATM_Hist/CFC_ATM_Hist_2015.]

Bullister, J. L., and D. P. Wisegarver (2008), The shipboard analysis of trace levels of sulfur hexafluoride, CFC11 and CFC12 in seawater, *Deep Sea Res., Part I*, *55*, 1063–1074, doi:10.1016/j.-dsr.2008.03.014.

Bullister, J. L., D. P. Wisegarver, and F. A. Menzia (2002), The solubility of sulfur hexafluoride in water and seawater, *Deep Sea Res., Part I*, *49*, 175–187.

Bullister, J. L., D. P. Wisegarver, and R. E. Sonnerup (2006), Sulfur hexafluoride as a transient tracer in the North Pacific Ocean, *Geophys. Res. Lett.*, *33*, L18603, doi:10.1029/2006GL026514.

Conkright, M. E., R. A. Locarnini, H. E. Garcia, T. D. O'Brien, T. P. Boyer, C. Stephens, and J. I. Antonov (2002), *World Ocean Atlas 2001: Objective Analyses, Data Statistics, and Figures* [CD-ROM], 17 pp., Natl. Oceanogr. Data Cent., Silver Spring, Md.

Doney S. C., and J. L. Bullister (1992), A chlorofluorocarbon section in the eastern North Atlantic, *Deep Sea Res., Part A*, *39*, 1857–1883.

Emerson, S., and C. Stump (2010), Net biological oxygen production in the ocean—II: Remote in situ measurements of O_2 and N_2 in subarctic Pacific surface waters, *Deep Sea Res., Part I*, *57*, 1255–1265.

Emerson, S., C. Stump, and D. Nicholson (2008), Net biological oxygen production in the ocean: Remote in situ measurements of O_2 and N_2 in surface waters, *Global Biogeochem. Cycles*, *22*, GB3023, doi:10.1029/2007GB003095.

Haine, T. W. N., and T. M. Hall (2002), A generalized transport theory: Water-mass composition and age, *J. Phys. Oceangr.*, *32*, 1932–1946.

Hall, T. M., T. W. N. Haine, and D. W. Waugh (2002), Inferring the concentration of anthropogenic carbon in the ocean from tracers, *Global Biogeochem. Cycles*, *16*(4), 1131, doi:10.1029/2001GB001835.

Hartin, C. A., R. A. Fine, B. M. Sloyan, L. D. Talley, T. K. Chereskin, and J. Happell (2011), Formation rates of Subantarctic mode water and Antarctic intermediate water within the South Pacific, *Deep Sea Res., Part I*, *58*, 524–534, doi:10.1016/j.dsr.2011.02.010.

Jenkins, W. J. (1987), ^{3}H and ^{3}He in the Beta Triangle: Observations of gyre ventilation and oxygen utilization rates, *J. Phys. Oceanogr.*, *17*, 763–783.

Kadko, D. (2009), Rapid oxygen utilization in the ocean twilight zone assessed with the cosmogenic isotope ^{7}Be, *Global Biogeochem. Cycles*, *23*, GB4010, doi:10.1029/2009GB003510.

Khatiwala, S., M. Visbeck, and P. Schlosser (2001), Age tracers in an ocean GCM, *Deep Sea Res., Part I*, *48*, 1423–1441.

Kim, I.-N., D.-H. Min, and A. M. MacDonald (2013), Water column denitrification rates in the oxygen minimum layer of the Pacific Ocean along 31°S, *Global Biogeochem. Cycles*, *27*, 816–827, doi:10.1002/gbc.20070.

Laws, E. A., P. G. Falkowski, W. O. Smith Jr., H. Ducklow, and J. J. McCarthy (2000), Temperature effects on export production in the open ocean, *Global Biogeochem. Cycles*, *14*(4), 1231–1246, doi:10.1029/199GB001229.

Letelier, R. M., D. M. Karl, M. R. Abbott, and R. R. Bidigare (2004), Light driven seasonal patterns of chlorophyll and nitrate in the lower euphotic zone of the North Pacific subtropical gyre, *Limnol. Oceanogr. Methods*, *49*, 508–519.

Martin, J. H., G. A. Knauer, D. M. Karl, and W. W. Broenkow (1987), VERTEX: Carbon cycling in the Northeast Pacific, *Deep Sea Res., Part A*, *34*(2), 267–285.

Mecking, S., M. J. Warner, C. E. Greene, S. L. Hautala, and R. E. Sonnerup (2004), Influence of mixing on CFC uptake and CFC ages in the North Pacific thermocline, *J. Geophys. Res.*, *109*, C07014, doi:10.1029/2003JC001988.

Mecking, S., M. J. Warner, and J. L. Bullister (2006), Temporal changes in pCFC-12 ages and AOU along two hydrographic sections in the eastern subtropical North Pacific, *Deep Sea Res., Part I*, *53*, 169–187.

Min, D.-H., J. L. Bullister, and R. F. Weiss (2002), Anomalous chlorofluorocarbons in the Southern California Borderland Basins, *Geophys. Res. Lett.*, *29*(20), 1955, doi:10.1029/2002GL015408.

Nicholson, D., S. Emerson, and C. Eriksen (2008), In situ determination of T, S, and O_2 in the subtropical North Pacific using glider surveys, *Limnol. Oceanogr. Methods*, *53*(5), 2226–2236.

Peacock, S., and M. Maltrud (2006), Transit-time distributions in a global ocean model, *J. Phys. Oceanogr.*, *36*, 474–495.

Quay, P. D., and J. Stutsman (2003), Surface layer carbon budget for the subtropical N. Pacific: δ^{13}C constraints at Station ALOHA, *Deep Sea Res., Part I*, *50*, 1045–1061, doi:10.1016/S0967-0637(03)0116-X.

Reuer, M. K., B. A. Barnett, M. L. Bender, P. G. Falkowski, and M. B. Hendricks (2007), New estimates of Southern Ocean biological production from O_2/Ar ratios and the triple isotope composition of O2, *Deep Sea Res., Part I*, *54*, 1853–1858.

Schlitzer, R. (2002), Carbon export fluxes in the Southern Ocean: Results from inverse modeling and comparison with satellite-based estimates, *Deep Sea Res., Part II*, *49*(9-10), 1623–1644, doi:10.1016/S0967-0645(02)00004-8.

Shao, A. E., S. Mecking, L. Thompson, and R. E. Sonnerup (2013), Mixed layer saturations of CFC-11, CFC-12, and SF_6 in a global isopycnal model, *J. Geophys. Res. Oceans*, *118*, 4978–4988, doi:10.1002/jgrc.20370.

Sonnerup, R. E. (2001), On the relations among CFC derived water mass ages, *Geophys. Res. Lett.*, *28*(9), 1739–1742.

Sonnerup, R. E., P. D. Quay and J. L. Bullister (1999a), Thermocline ventilation and oxygen utilization rates in the subtropical North Pacific based on CFC distributions during WOCE, *Deep Sea Res., Part I*, *46*, 777–805.

Sonnerup, R. E., P. D. Quay, A. P. McNichol, J. L. Bullister, T. A. Westby, and H. L. Anderson (1999b), Reconstructing the oceanic ^{13}C Suess effect, *Global Biogeochem. Cycles*, *13*(4), 857–873.

Sonnerup, R. E., J. L. Bullister, and S. Mecking (2007), Circulation rate changes in the eastern subtropical North Pacific based on chlorofluorocarbon ages, *Geophys. Res. Lett.*, *34*, L08605, doi:10.1029/2006GL028813.

Sonnerup, R. E., J. L. Bullister, and M. J. Warner (2008), Improved estimates of ventilation rate changes and CO_2 uptake in the Pacific Ocean using chlorofluorocarbons and sulfur hexafluoride, *J. Geophys. Res.*, *113*, C12007, doi:10.1029/2008JC004864.

Sonnerup, R. E., S. Mecking, and J. L. Bullister (2013), Transit time distributions and oxygen utilization rates in the Northeast Pacific Ocean from chlorofluorocarbons and sulfur hexafluoride, *Deep Sea Res., Part I*, *72*, 61–71, doi:10.1016/j.dsr.2012.10.013.

Stanley, R. H. R., S. C. Doney, W. J. Jenkins, and D. E. Lott III (2012), Apparent oxygen utilization rates calculated from tritium and helium-3 profiles at the Bermuda Atlantic Time-series Study site, *Biogeosciences*, *9*, 1969–1983, doi:10.5194/bg-9-1969-2012.

Stommel, H. M. (1979), Determination of water mass properties of water pumped down from the Ekman layer to the geostrophic flow below, *Proc. Natl. Acad. Sci. U. S. A.*, *97*, 2051–3055.

Tanhua, T., D. W. Waugh, and D. W. R. Wallace (2008), Use of SF_6 to estimate anthropogenic CO_2 in the upper ocean, *J. Geophys. Res.*, *113*, C04037, doi:10.1029/2007JC004416.

Tanhua, T., D. W. Waugh, and J. L. Bullister (2013), Estimating changes in ocean ventilation from early 1990s CFC-12 and late 2000s SF_6 measurements, *Geophys. Res. Lett.*, *40*, 927–932, doi:10.1002/grl.50251.

Warner, M. J., and R. F. Weiss (1985), Solubilities of chlorofluorocarbons 11 and 12 in water and seawater, *Deep Sea Res., Part A*, *32*, 1485–1497.

Warner, M. J., and R. F. Weiss (1992), Chlorofluoromethanes in South Atlantic Antarctic Intermediate Water, *Deep Sea Res., Part A*, *39*(11/12), 2053–2075.

Warner, M. J., J. L. Bullister, D. P. Wisegarver, R. H. Gammon, and R. H. Weiss (1996), Basinwide distributions of chlorofluorocarbons CFC-11 and CFC-12 in the North Pacific: 1985–1989, *J. Geophys. Res.*, *101*(C9), 20,525–20,542.

Waugh, D., and T. Hall (2002), Age of stratospheric air: Theory, observations, and models, *Rev. Geophys.*, *40*(4), 1010, doi:10.1029/2000RG000101.

Waugh, D. W., M. K. Vollmer, R. F. Weiss, T. W. N. Haine, and T. M. Hall (2002), Transit time distributions in Lake Issyk-Kül, *Geophys. Res. Lett.*, *29*(24), 2231, doi:10.1029/2002GL016201.

Waugh, D. W., T. M. Hall, and T. W. N. Haine (2003), Relationships among tracer ages, *J. Geophys. Res.*, *108*(C5), 3138, doi:10.1029/2002JC001325.

Waugh, D. W., T. W. N. Haine, and T. M. Hall (2004), Transport times and anthropogenic carbon in the subpolar North Atlantic Ocean, *Deep Sea Res., Part I*, *51*, 1475–1491.

Waugh, D. W., F. Primeau, T. DeVries, and M. Holzer (2013), Recent changes in the ventilation of the Southern Oceans, *Science*, *339*(6119), 568–570, doi:10.1126/science.1225411.